Pressure effects on the initial carbonization reactions of anthracene

P W Whang, F Dachille, P L Walker Jr
Materials Research Laboratory and Department of Material Sciences, Pennsylvania State University, University Park, Pennsylvania 16802, USA

Abstract. A study of the thermal conversion of anthracene to a carbonaceous solid at temperatures between 490 and 509°C and pressures between 0·34 and 2·07 kbar has been made. The rate of disappearance of anthracene in the early stages of carbonization has been followed. The rate increases with pressure and obeys first-order kinetics, with an activation energy of 22·5 kcal mol^{-1} and activation volume of -17 cm^3 mol^{-1}, over the pressure range from 1·38 to 2·07 kbar. This low activation energy and a negative activation volume are taken to be indicative of the role played by paramagnetic species produced by the formation of π-complexes with anthracene. The initial carbonization step includes a process forming the polymeric species. The mono- and biradical of anthracene, rather than anthracene, appear to lead directly to the formation of the polymeric products. As shown by mass spectrometric analyses of the solid products, subsequent condensation to large aromatic molecules is favored through the formation of reactive alkyl aromatics and/or methylene bridged aromatics.

1 Introduction

The physicochemical changes which take place during carbonization are extremely complex. Nevertheless, the carbonization at atmospheric pressure of anthracene, among many organic compounds, has been extensively studied by Kinney (1956), Kinney et al. (1958), Madison and Roberts (1958), Walker and Weinstein (1967), and Weintraub and Walker (1971). Most of these investigations have been concerned with the graphitizing character of the resulting carbon. On the other hand, Singer (1969) and Lewis and Singer (1969) have examined the hyperfine ESR signals coming from intermediates produced during the carbonization of various aromatic compounds. For anthracene, Lewis (1973a) concludes that polymerization occurs at the reactive 9,10-positions leading to the formation of bianthryl, dibenzoperylene, and bisanthene. Dibenzoperylene and bisanthene, as well as anthracene, have been identified following liquid phase pyrolysis of 9,9'-bianthryl.

In the present work a study has been made of the influence of pressure on the carbonization of anthracene. This investigation was restricted to reactions taking place in the early stages, because with increasing reaction time, the complexity and plurality of products having especially high molecular weight make an interpretation difficult. The use of the pressure variable in the carbonization system is perhaps one of the more fruitful methods for clarifying the reaction process, because chemical equilibrium and reaction rates are strongly dependent on pressure as well as temperature.

2 Experimental

2.1 Materials

Anthracene manufactured by Aldrich Chemical Company was used in this study. It had a purity greater than 99·9% and a melting point at atmospheric pressure of 215–217°C. This compound was not further purified. Xylene of reagent grade from J. T. Baker Chemical Company was employed as a solvent, without further purification, for extraction. Gold tubes from Matthey Bishop Company of purity greater than 99·994% were used as sample containers during carbonization.

Advantages in using gold tubes are its chemical inertness, ease of welding, and malleability for allowing the pressure applied to be transmitted directly to the sample.

2.2 Carbonization procedure

Anthracene was pressed into cylindrical tablets (4 mm diameter, ~15 mm long, weighing ~0·25 g) for easy handling and then was packed in gold tubes. Tubes containing the samples were sealed off under a nitrogen atmosphere with the aid of a carbon-arc welder. Carbonization of anthracene was then carried out in a hydrothermal pressure vessel into the bottom of which the gold tube, containing the sample tablets, was loaded as shown in figure 1. Desired pressures were applied to the gold tubing by a hydraulic compressor with demineralized water used as the transmitting medium. The pressure was controlled automatically within ±35 bar during the period of heating. In order to conduct isothermal carbonizations to obtain kinetic data, the pressure vessel was plunged into the furnace preheated to about 850°C. With the use of this plunge heating the final desired reaction temperatures were attained within ≤7 min.
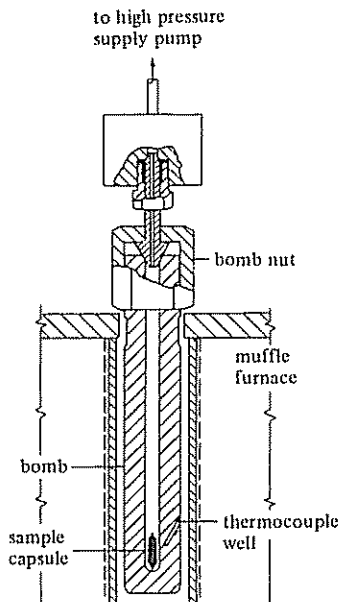

Figure 1. Cold seal pressure vessel.

2.3 Mass spectrometric analyses

The gaseous and solid products of carbonization were analyzed by an AEI MS 9 mass spectrometer. Prior to the analyses, tubes containing carbonized products were punctured in a closed system which had previously been evacuated in order to collect the gaseous products. The pressure of the gases expanded into the known volume was measured. The mass spectrometer was equipped with a heated inlet system, capable of vaporizing solid samples at temperatures up to about 300°C. The energy of the electron beam used for gas analyses was set at 70 eV, which exceeded the energy required to produce molecular ions. The mass spectra of the solid products were obtained using low energy electrons (12 eV) according to the low-ionizing-voltage technique described by Lumpkin (1958) aimed at producing spectra that consist only of molecular ions.

2.4 *Infrared absorption analyses*

Infrared spectra of carbonized solid products were obtained on a Perkin–Elmer 621 grating infrared spectrophotometer by established procedures with KBr pellets containing 0·2 wt.% of the sample.

2.5 *Measurement of* ESR *spectra*

ESR spectra of carbonized solid products were obtained in terms of the first derivative curve by a Perkin–Elmer Model ESR-1 electron spin resonance spectrometer. The g-values were measured in relation to the known g-value of standard DPPH (diphenyl picryl hydrazyl) from the difference in the resonance field strength. Spin concentrations were determined by measuring the areas of the first derivative curves and then comparing these areas with a standard curve which was obtained from standard solutions of DPPH. Line widths were obtained by measuring the distance from peak to peak in the first derivative curves.

2.6 *Analysis for anthracene*

In order to follow the rate of disappearance of anthracene, the amount of reactant left following a carbonization reaction was determined from UV absorption spectra as measured with a Beckman DK 2A spectrophotometer. A known amount of the solid product was first extracted with xylene in a Soxhlet extraction apparatus. The extracted soluble portion was diluted to a standard volume and used to obtain the UV spectra at wavelengths between 350 and 400 nm. The peak height at 376 nm was compared with a calibration curve obtained by the base line method (Hazlett *et al.*, 1950). This method assumes that the extraneous background absorption due to many carbonized products is linear. In practice, linear absorption curves were confirmed to exist between 350 and 400 nm.

3 Results

3.1 *Pressure effects on the rates of thermal conversion*

The thermal conversion of anthracene in the initial period of reaction was found to follow first-order kinetics. That is, plots of the logarithm of the ratio of the initial weight of anthracene to the weight at time t versus t were straight lines (figure 2).
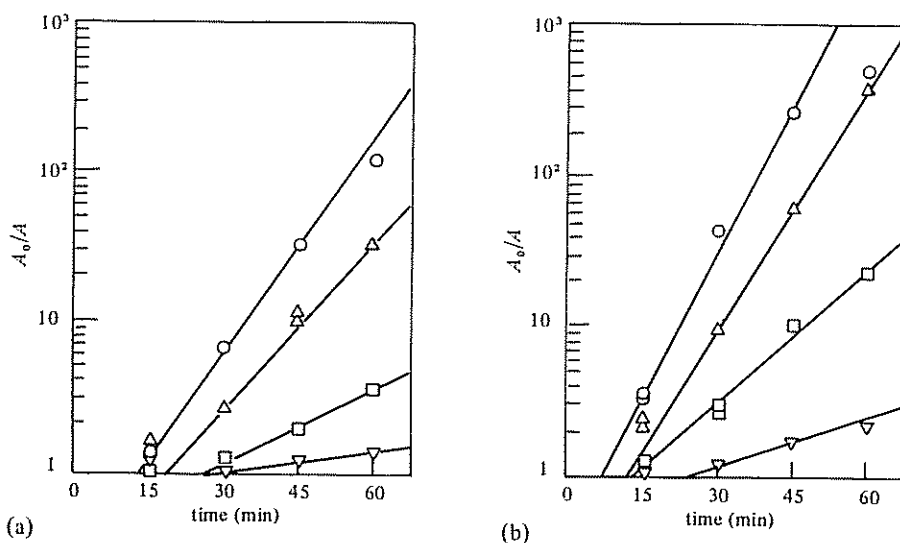
Figure 2. First-order kinetic plots for the disappearance of anthracene at (a) 490°C and (b) 509°C under different pressures (kbar): ▽, 0·34; □, 0·68; △, 1·36; ○, 2·07.

Induction periods were found under all conditions. Table 1 summarizes the kinetic data where first-order rate constants, k, activation energies, E_a, and preexponential factors, A, were calculated from slopes of the first-order plots and the Arrhenius equation, respectively. The volume of activation, $\Delta V^{\ddagger}$, was calculated over the pressure range from 1·36 to 2·07 kbar from the expression

$$\left(\frac{\partial \ln k}{\partial P}\right)_T = -\frac{\Delta V^{\ddagger}}{RT} \, ,$$

where the partial derivative on the left-hand side could be obtained from the slope of plots such as shown in figure 3.

Table 1. Kinetic data on the disappearance of anthracene during carbonization.

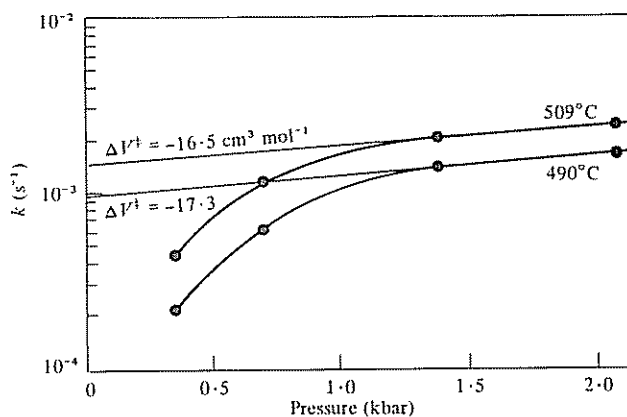| Pressure (kbar)	k (s^{-1})		E_a (kcal mol^{-1})	A (s^{-1})
	490°C	509°C		
0·34	$2\cdot18 \times 10^{-4}$	$4\cdot53 \times 10^{-4}$	45·7	$2\cdot6 \times 10^{9}$
0·68	$6\cdot29 \times 10^{-4}$	$1\cdot16 \times 10^{-3}$	38·2	$5\cdot5 \times 10^{7}$
1·36	$1\cdot46 \times 10^{-3}$	$2\cdot10 \times 10^{-3}$	22·7	$4\cdot6 \times 10^{3}$
2·07	$1\cdot77 \times 10^{-3}$	$2\cdot53 \times 10^{-3}$	22·3	$4\cdot3 \times 10^{3}$

Figure 3. Influence of pressure on the first-order rate constants for the disappearance of anthracene upon carbonization at 490 and 509°C.

3.2 Pressure effects on the path of the thermal conversion

3.2.1 Infrared results.
Figure 4 shows the IR spectra of untreated anthracene and products resulting from the heating of anthracene at 490°C for 15 min under various pressures. The IR spectra of anthracene carbonized at 509°C under pressure are generally similar to those obtained at 490°C, except for a greater reduction in peak intensities per unit of reaction time.

As pressure is increased, while the other conditions are held constant, a new IR band commences to appear at 2900–2920 cm^{-1}, indicating the presence of an aliphatic C–H stretching vibration. Weak bands between 1787 and 1950 cm^{-1} are usually assigned to overtones and combination tones which disappear rather rapidly as reaction proceeds. Bands in the 1286–1623 cm^{-1} region are caused by aromatic ring stretching vibrations. Their shift and broadening upon carbonization become evident; for example, note the progressive broadening of the 1623 cm^{-1} peak. This perhaps is a result of the presence of quinoid structure. The band at 906 cm^{-1} shows a steady decrease in its intensity as pressure is increased and completely disappears following carbonization at 2·07 kbar for 15 min. This is due to loss of

aromatic character in the 9,10-positions of anthracene as a result of substitutions in these positions (Cannon and Sutherland, 1951). The distinct IR bands at 886 and 729 cm^{-1} remain even after carbonization at the highest pressures. They are both characteristic of the IR spectra of anthracene and its polymeric products. The analysis of the IR spectra obtained in this investigation suggests that reaction proceeds through 9,10-positions, possibly with the formation of quinoid structures.
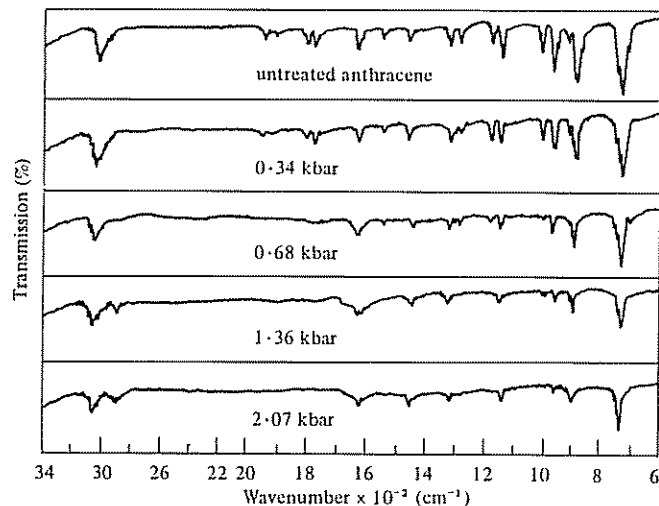

Figure 4. Infrared spectra of products from anthracene upon carbonization at various pressures at 490°C for 15 min.

3.2.2 *Mass spectrometric results.* Mass spectra of solid products at ionization voltages of both 12 and 70 eV showed basically the same species at masses above 178. However, the spectra from 70 eV showed many species having masses less than 178, while the spectra from 12 eV showed few species below 178. Therefore most species appearing below m/e = 178, at 70 eV, were considered to be produced by fragmentation of species of larger mass in the ionization chamber. Generally, the spectra consist of several groups of peaks, each group being separated substantially from neighboring groups. Each group is composed of five to eight peaks, the separation between peaks being one unit of m/e. Table 2 lists the m/e values in groups for convenience. The parent molecular species proposed is given on the assumption that each group of peaks is represented by one parent molecule. Presumably there may be higher polymeric species than those observed in the spectra, but their vapor pressures would be too low to be detected at chamber temperatures between 270–300°C. An earlier study by Evans (1969) showed that, at temperatures below 500°C under normal pressure, pyrolysis of anthracene with the formation of compounds of higher molecular weight essentially did not occur. From this study it is obvious, however, that application of pressure lowers the temperatures at which carbonization of anthracene leads to formation of higher molecular-weight species.

Table 3 lists the mass numbers of solid products obtained by isothermal carbonization for 1 h under pressures of 0·68 and 1·36 kbar. One interesting sequence is observed in the masses. It is frequently evident that masses from one peak to the next include the interval of 12 or 14 mass units. This is taken as evidence that molecules increase in weight by increments of (CH$_2$) units.

Following some runs, the gold tubes were punctured and the gaseous product expanded into a known volume. From the pressure of the expanded gas (which in

Table 2. Mass spectrometric data from the solid resulting from the carbonization of anthracene at 490°C for 15 min under various pressures.

m/e values	Relative intensity for pressures (kbar)[a]				Proposed parent species for each group
	2·07	1·36	0·68	0·34	
128	w	w	w	w	naphthalene
142	w	w	w	w	methyl-naphthalene
156	w	w	w	w	dimethyl-naphthalene
174	w	w	w	w	
175	w	w	w	w	
176	w	m	m	m	
177	w	m	m	m	(monomer)
178	vs	vs	vs	vs	
179	m	m	m	m	
180	w	m	m	m	
350	w	m	m	m	
351	w	w	w	m	
352	m	m	s	s	
353	m	s	m	m	(dimer)
354	m	s	w	w	
355	w	m	w	w	
356	-	w	-	-	
526	s	-	-	-	
527	m	-	-	-	
528	vs	m	w	-	
529	vs	w	w	-	(trimer)
530	vs	s	s	m	
531	m	m	m	w	
532	m	w	w	w	
700	w	w	-	-	(tetramer)
715[b]	m	m	-	-	

Abbreviations: vs = very strong, s = strong, m = medium, w = weak.

[a] Ionization chamber temperature 270–300°C, ionization voltage 12 eV
[b] Masses also present between 700–715

Table 3. Mass spectrometric data from the solid resulting from the carbonization of anthracene at 509°C for 60 min under various pressures.

Carbonization pressure (kbar)	m/e values and relative intensities[a]
0·68	178(s), 179(w), 182(m), 192(s), 193(w), 196(w), 206(m), 218(w), 220(w), 228(w), 230(w), 232(w), 242(w), 244(w), 252(w), 254(w), 266(w), 272(w), 278(m), 280(w), 292(w), 294(w), 302(m), 304(m), 342(m), 344(m), 352(s), 354(s), 356(s), 358(m), 366(m), 368(m), 380(w), 390(w), 402(w), 404(w), 416(w), 418(w), 426(w), 428(w), 440(w), 442(w), 452(w), 454(w), 466(w), 476(w), 478(w), 490(w), 492(w), 502(w), 504(w), 506(w), 514(w), 516(w)
1·36	128(m), 142(s), 156(w), 178(s), 192(m), 206(m), 213(m), 224(m), 225(m), 226(m), 238(m), 252(s), 266(m), 278(m), 280(w), 302(s), 316(m), 328(w), 330(m), 352(s), 366(m), 376(w), 390(w), 404(m), 416(w), 426(m), 440(m), 452(m), 454(s), 466(m), 478(s), 492(s), 504(m), 506(m), 516(m), 530(m)

Abbreviations: s = strong, m = medium, w = weak.
[a] Ionization chamber temperature 270–300°C, ionization voltage 12 eV

all cases was less than 1 atm), the moles of gaseous product could be estimated from the ideal gas law. Table 4 summarizes results for carbonization runs at 500°C and 0·52 kbar. Also shown are the moles and percentage of anthracene disappearing as a function of time. It is seen that, for short reaction times, the moles of anthracene disappearing greatly exceed the moles of gas produced (by a factor of about 100). However, for reaction times greater than $\frac{1}{2}$ h the rate of anthracene disappearance falls off much more sharply with increasing time than does the rate of gas production. As a consequence, following reaction for 10 h, the cumulative value of the moles of gas produced approaches the cumulative value of the moles of anthracene reacted. Gaseous species identified from mass spectrometric analyses were hydrogen, methane, ethane, propane, butane, and butene in trace amounts. For a $\frac{1}{4}$ h reaction time, hydrogen and methane were present in essentially equal amounts. But, as reaction time proceeds, methane becomes the abundant species. For a reaction time of 22 h, the average molecular weight of the gas, calculated from the moles of gas and loss in container, and sample weight following puncturing the container, was approximately 20.

Table 4. Gas produced and anthracene decomposed during carbonization at 500°C and 0·52 kbar.

Reaction time (h)	Product gas (moles)	Anthracene decomposed		$\dfrac{m_g{}^a}{m_a}$
		(moles)	(%)	
$\frac{1}{4}$	$5·2 \times 10^{-6}$	$5·3 \times 10^{-4}$	42·6	0·010
$\frac{1}{2}$	$1·0 \times 10^{-5}$	$9·8 \times 10^{-4}$	67·0	0·010
$\frac{3}{4}$	$6·2 \times 10^{-5}$	$1·1 \times 10^{-3}$	81·0	0·056
1	$2·0 \times 10^{-4}$	$1·3 \times 10^{-3}$	89·1	0·15
3	$7·9 \times 10^{-4}$	$1·4 \times 10^{-3}$	99·8	0·57
10	$1·1 \times 10^{-3}$	$1·4 \times 10^{-3}$	~100	0·79
22	$1·1 \times 10^{-3}$	$1·5 \times 10^{-3}$	~100	0·74

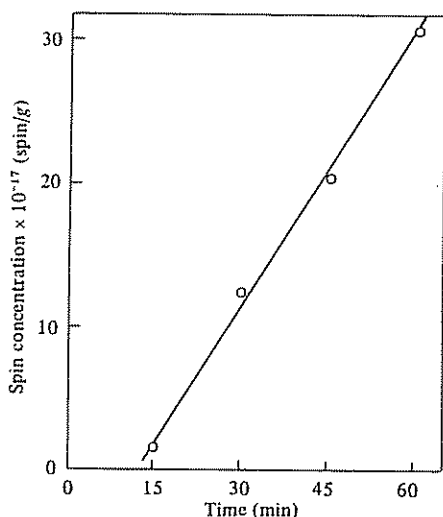$$^a \quad \frac{m_g}{m_a} = \frac{\text{moles gas produced}}{\text{moles anthracene decomposed}}$$

Figure 5. Influence of reaction time on the formation of paramagnetic species upon the carbonization of anthracene at 1·36 kbar and 490°C.
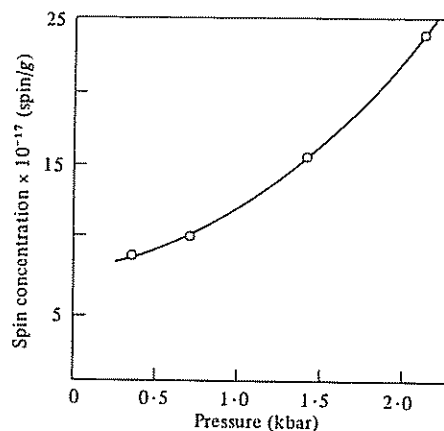
Figure 6. Influence of pressure on the formation of paramagnetic species upon the carbonization of anthracene at 490°C for 15 min.

3.2.3 ESR *results*. Figures 5, 6, and 7 summarize ESR results for carbonization at 490°C. It is seen from figure 5 that for carbonization under 1·36 kbar pressure the spin concentration of the solid product increases continually with reaction time. From figures 6 and 7 it is seen that for carbonization for 15 min the spin concentration increases, *g*-value decreases, and line width increases with increasing reaction pressure.
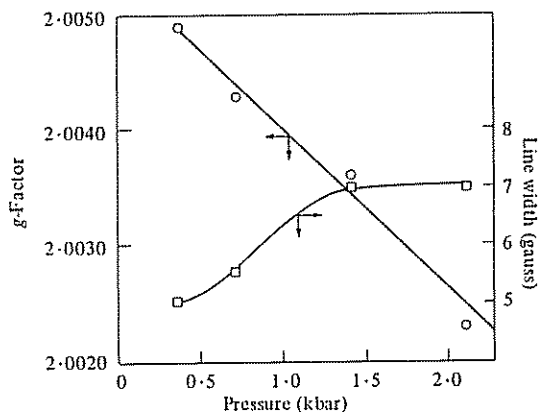

Figure 7. Variation of *g*-factor and line width of ESR spectra from paramagnetic species formed at various pressures during the carbonization of anthracene at 490°C for 15 min.

4 Discussion

As seen in table 2, species having masses of 176, 177, 179, and 180 occurred in considerable abundance during the early stages of carbonization of anthracene at 490°C. At the same time, as seen in table 4, the formation of gaseous products during the early stages of carbonization was limited. These results suggest that radical species are formed from bimolecular processes as follows

(1)

(2)
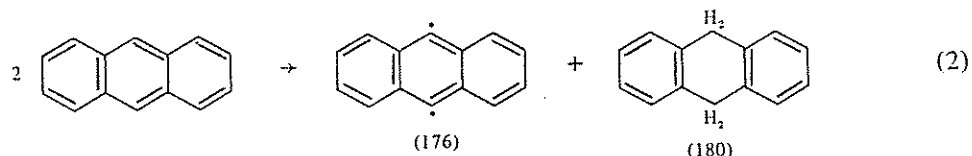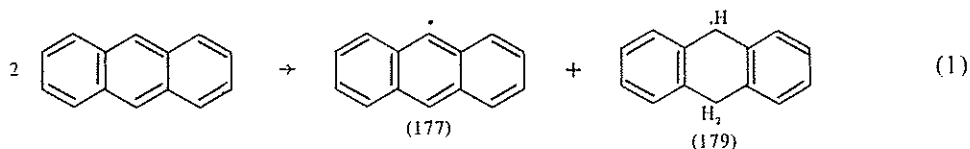
where the numbers in parentheses indicate mass numbers. Both proposed reactions produce no hydrogen. Anthryl radicals can then react to form 9,9'-bianthryl, which upon loss of hydrogen can ultimately lead to bisanthene:

(3)
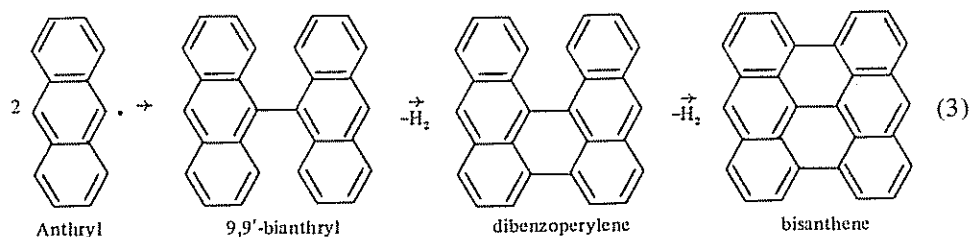
Dibenzoperylene and bisanthene have been identified by Lewis (1973b) from the liquid phase pyrolysis of 9,9'-bianthryl at 440°C. Lewis further proposes that the following polymer structure is a subsequent reaction product
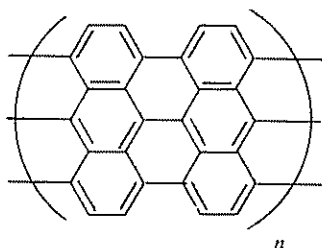

(4)

For carbonization of anthracene at 500°C Lewis suggests that $n \approx 2$ and that one unpaired electron is expected per polymer unit.

It is thus understandable that a negligible amount of hydrogen is found in the gaseous reaction products and that methane is by far the predominant gaseous product: the hydrogen released in the conversion of anthracene to the above polymer structure would in turn be expected to react with hydroaromatic structures like dihydroanthracene leading eventually to the most stable hydrocarbon, methane.

It is interesting to speculate further on the initial reactions involved in the conversion of aromatic hydrocarbons to polymeric products and eventually to carbon. It is known that there are major differences in the rates at which hydrocarbons undergo liquid phase pyrolysis. For example, Weintraub and Walker (1971) found the pyrolysis rates of three hydrocarbons which they studied to be in the order: anthracene $\gg$ phenanthrene $>$ biphenyl. It is thought to be significant that, in turn, the excitation energies for the ground singlet–triplet transition for these three molecules are: anthracene, $42 \cdot 1$ kcal mol^{-1}; phenanthrene, $61 \cdot 8$ kcal mol^{-1}; and biphenyl $65 \cdot 2$ kcal mol^{-1}, as given by Szwarc (1955). This suggests that the rate of this transition may be the slow step in the over-all reaction of aromatic to polymer.

In this regard the production of paramagnetic species during the carbonization of anthracene takes on additional significance. Berlin *et al.* (1964), for example, suggested that paramagnetic species, which initially may be present in anthracene as impurities or induced therein during pressure carbonization, can serve as catalysts for the acceleration of radical polymerization by forming π-complexes with diamagnetic species. More specifically, the formation of π-complexes between paramagnetic species and anthracene would be expected to increase the probability (rate) of transition of anthracene molecules from a ground singlet state to a triplet state. A comparison of the activation energy for anthracene disappearance at pressures above $1 \cdot 36$ kbar, 22 kcal mol^{-1}, with the excitation energy for the singlet–triplet transition in anthracene, $42 \cdot 1$ kcal mol^{-1}, suggests that the mode of catalysis may be by a significant lowering of the activation energy for the transition when an activated complex is formed between anthracene and a paramagnetic species. It would be expected that following the transition of anthracene molecules to the triplet state, the rate of reactions (1) and (2) would be markedly accelerated.

As to the structure of the polymeric products, the presence of quinoid structure was also suggested from the broadening of the IR band from 1600 to 1650 cm^{-1} for samples carbonized above $1 \cdot 36$ kbar. The quinoid structure implies that the biradical of anthracene also participates in the formation of polymeric species. It is suggested that the general structure of the quinoid species is as follows:
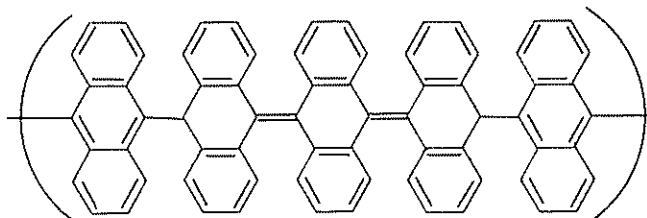
$$(5)$$

The two individual spins in a biradical are expected to exist in a triplet state so that the reactivity will be much enhanced. Szwarc (1948) pointed out that the formation of a high polymer in the pyrolysis of xylene should be ascribed to the presence of a biradical which forms from p-xylene rather than o- or m-xylene.

5 Conclusions

Initial carbonization reactions of anthracene are thought to involve primarily the formation of anthryl radicals at the 9 and 10 positions followed by polymerization. Formation of anthryl radicals is considered to be preceded by the transition of anthracene molecules in the ground singlet state to the triplet state. This transition is expected to be catalyzed by paramagnetic species. It is shown that, in turn, as carbonization of anthracene proceeds the concentration of paramagnetic species increases. The rates of disappearance of anthracene and appearance of paramagnetic species increase as carbonization is carried out at increasing pressures. Thus it is concluded that pressure accelerates the rate of the ground singlet–triplet transition in anthracene molecules, probably by enhancing the interaction of anthracene molecules with paramagnetic species to form π-complexes.

References
Berlin, A. A., Grigorovskaya, V. A., Parini, V. P., Gafurov, Kh., 1964, *Dokl. Akad. Nauk SSSR*, 156, 1371–1374.
Cannon, C. G., Sutherland, G. B. B. M., 1951, *Spectrochim. Acta*, 4, 373–395.
Evans, S., 1969, Ph. D. Thesis, The University of Newcastle upon Tyne, England.
Hazlett, F. P., Hannan, R. B., Jr., Wells, J. H., 1950, *Anal. Chem.*, 22, 1132–1136.
Kinney, C. R., 1956, *Proceedings of the First and Second Carbon Conference* (University of Buffalo), pp.83–92.
Kinney, C. R., Nunn, R. C., Walker, P. L., Jr., 1958, *Ind. Eng. Chem.*, 49, 880–884.
Lewis, I. C., Singer, L. S., 1969, *158th Meeting of ACS, Division of Fuel Chem.*, 13, 86–100.
Lewis, I. C., 1973a, *Spring Meeting of ACS, Division of Polymer Chemistry*, 14, 380–392.
Lewis, I. C., 1973b, private communication.
Lumpkin, H. E., 1958, *Anal. Chem.*, 30, 321–325.
Madison, J. J., Roberts, R. M., 1958, *Ind. Eng. Chem.*, 50, 237–250.
Singer, L. S., 1969, *J. Chim. Phys.*, Special Number, April, 21–27.
Szwarc, M., 1948, *J. Chem. Phys.*, 16, 128–136.
Szwarc, M., 1955, *J. Chem. Phys.*, 23, 204–206.
Walker, P. L., Jr., Weinstein, A., 1967, *Carbon*, 5, 13–17.
Weintraub, A., Walker, P. L., Jr., 1971, *Proceedings of the Third Conference on Industrial Carbon and Graphite* (Society of Chemical Industry, London), pp.75–83.